Master of Science Thesis:

Real-time dynamic MLC tracking for inversely optimised arc radiotherapy

Marianne Falk

Supervisors:
Per Munck af Rosenschöld
Stine Korreman

The work has been performed at the Department of Radiation Physics at Rigshospitalet, Copenhagen, Denmark

Medical Radiation Physics
Clinical Sciences, Lund
Lund University, 2009

Marianne Falk

Rotations- strålbehandling anpassad för tumörens rörelser

Strålbehandling är en vanlig behandlingsform av cancer. Röntgenstrålning med mycket hög energi riktas mot behandlingsområdet och slår ut cancerceller. Strålningen påverkar även friska celler men i allmänhet i mindre grad. Det är därför önskvärt att minimera stråldosen till frisk vävnad utan att för den skull riskera att missa tumörceller. Detta kan vara en svår uppgift då tumören rör sig under behandlingen som t ex lungtumörer som förflyttar sig då patienten andas. I dag behandlas vanligen en stor del frisk lunga för att man vill vara säker på att tumören befinner sig i behandlingsvolymen under hela behandlingen, även om den flyttar på sig. Då lungcancerpatienter ofta har nedsatt lungfunktion är det av stor vikt att undvika att bestråla frisk lungvävnad i största möjliga mån då detta påverkar lungorna negativt.

Förutom strålkällan sitter en dynamisk multibladskollimator (*DMLC*) monterad i apparaten. DMLC:n består av rörliga metallblad som efter en förbestämd patientspecifik plan formar strålfältet för att behandla tumören på ett lämpligt sätt. I detta examensarbete studerades en ny teknik där DMLC:n ändrar form i enighet med tumörens rörelser, s.k. *DMLC tracking*. Realtidsinformation om tumörens position erhålls från ett system där infrarött ljus reflekteras av en markör med samma rörelsemönster som tumören. Med denna teknik skulle man potentiellt kunna minska den bestrålade lungvolymen och ändå få en fullgod behandling av cancern. Forskning av denna metod pågår och den används ännu inte kliniskt. Metoden har tidigare visat på gott resultat tillsammans med enklare strålbehandlingsmetoder. I detta arbete har undersökningar gjorts för DMLC trackings effekter på en ny behndlingsmetod, *RapidArc*.

RapidArc är en ny strålbehandlingsteknink där behandlingen ges under en rotation av strålkällan runt behandlingsområdet. Metoden har visat på goda behandlingsegenskaper, en förkortad behandlingstid och den används kliniskt på Rigshospitalet i Köpenhamn.
I examensarbetet studerades framför allt DMLC tracking metodens förmåga att kompensera för tumörrörelser i 1D av olika storlek och hurvida riktningen på DMLC bladens rörelsebana påverkar metodens utfall.

Resultaten visade att då behandlingsområdet rör sig under strålbehandlingen kan DMLC tracking koncentrara stråldosen bättre runt det område som är avsett jämfört med om man inte kompenserar för tumörrörelserna. Detta leder till slutsatsen att DMLC tracking möjliggör en mer nogrann behandling där stråldosen hamnar i den volym där den var avsedd trots att behandlingsområdet rör på sig. Detta skulle potentiellt kunna möjliggöra minskning av den volym av intilliggande frisk vävnad som bestrålas för att säkerställa att tumören får den önskade stråldosen. Studien visade inte på någon signifikant skillnad i DMLC tracking metodens prestationsförmåga beroende på storleken av tumörens rörelse eller DMLC bladens rörelseriktning. Stabiliteten i monitoreringssystemet som övervakar behandlingsområdets rörelser visade sig däremot vara otillräcklig för DMLC tracking. Andra kliniskt använda monitoreringssystem har testats med DMLC tracking med lovande resultat.

Handledare: **Per Munck af Rosenschöld, Stine Korreman**
Examensarbete 30 hp i Strålterapi 2009
Medicinsk strålningsfysik, Institutionen för kliniska vetenskaper , Lunds universitet

Marianne Falk

Real-time dynamic MLC tracking for inversely optimised arc radiotherapy

Purpose: Radiotherapy of moving tumours is a great challenge in cancer treatment. The moving target will lead to "dose-smearing" of the planned dose distribution and a need for larger margins. To reduce the dose to the surrounding healthy tissue, while still ensuring full coverage of the target, other methods for motion compensation is needed. Inversely optimised arc radiotherapy, where the treatment is delivered continuously during one (or several) gantry rotation(s), requires special consideration when choosing a motion compensation technique. Methods that assert beam holds (e.g. clinically used respiratory gating) are not an option since this compromises the delivery accuracy and efficiency. DMLC tracking is a method that uses the multileaf collimator (MLC) leaves to reposition according to the movements of the target. This may be an adequate motion compensation method for arc radiotherapy since it avoids beam holds during the treatment. The purpose of this study was to evaluate the performance of the DMLC tracking method together with inversely optimized arc radiotherapy with special attention on its dependence on varying peak to peak displacement and collimator angles.

Methods and materials: To simulate respiratory movements of the target, a 1D motion platform was programmed to form sinusoidal motion with peak to peak distances of 5 mm, 10 mm, 15 mm, 20 mm and 25 mm in the SI direction and a cycle time of 6 seconds. The DMLC-tracking system used 3D target position information from a Real-time Position Management™ (RPM) System (Varian Medical Systems, Palo Alto, CA) to reposition the MLC leaves to account for target displacements. Varian Medical Systems implementation of the inversely optimized arc radiotherapy technique (RapidArc™) was used for this study. Two RapidArc plans with collimator angle 45° and one plan with collimator angle 90° were created in Eclipse™ (Aria ver. 8.5) and delivered to the Delta-4 dosimetric system (Scandidos) with 6 MV using a Varian 2300ix Clinac. The gantry rotation angle was set to run from 210° to 150° to prevent intersection of the incoming beam and the rails of the couch. Measurements were made with the tracking system connected to the MLC as described above and with the tracking system disconnected, not affecting the plan delivery. Gamma index evaluation (3% dose difference, 3 mm DTA and 2% dose difference, 2 mm DTA), with static target measurements as references, were used to evaluate the results.

Results: The measurements where DMLC tracking were used showed a significant improvement of the delivery accuracy and a clear reduction of the dose smearing effects compared to the measurements where no motion compensation was used. No significant decrease in the tracking performance for increasing peak to peak displacement was seen. There was a small trend of better tracking performance with 90° collimator angle than for the measurements with 45°. Due to instabilities in the RPM system, some of the dose profiles were shifted which had a worsening effect on the tracking performance.

Conclusion: DMLC tracking can improve the accuracy of RapidArc delivery on a moving target. The method evaluated in this work was independent of the size of the peak to peak displacement of the target and works well with both 45° and 90° collimator angles. The use of a more reliable position monitor with DMLC tracking is warranted.

Advisors: **Per Munck af Rosenschöld, Stine Korreman**
Degree project 30 credits in Radiotherapy 2009
Department of Medical Radiation Physics, Clinical Sciences, Lund University

Table of contents

Abbreviations

AAA	Anisotropic Analytical Algorithm
CP	Control Points
DMLC	Dynamic Multi Leaf Collimator
DTA	Distance to agreement
IMAT	Intensity Modulated Arc Therapy
IMRT	Intensity Modulated Radiation therapy
k(t,p)	Correction factor for temperature and pressure
MLC	Multi Leaf Collimator
MU	Monitor Units
OAR	Organ At Risk
p-Si	P-doped Silicon
PRO	Progressive Resolution Optimisation
PTV	Planning Target Volume
QA	Quality Assurance
RT	Radiotherapy
SI	Superior-Inferior
TPS	Treatment Planning System
VMAT	Volumetric Modulated Arc Therapy

1. Introduction

Cancer treatment using inversely optimized arc radiotherapy is a novel treatment technique in radiotherapy. Intensity modulated arc therapy (IMAT) was first proposed by Yu et al [1] as multiple superimposed sub-fields created from two-dimensional beams and delivered as multiple arcs. The technique was refined by Otto [2] where it was referred to as VMAT. VMAT plans are created using inverse optimization and delivered with variation in dose rate, gantry speed and MLC shapes. Varian Medical Systems has a clinical implementation of the VMAT technique, RapidArc^{TM}, which was used in this study.

Lung cancer is the fifth most common cancer disease in Sweden and it is related to smoking, asbestos, radon and other environmental factors [3]. The disease is more common among men than among women but the difference decreases as a generation of frequently smoking women reaches the age where the cancer symptoms can be detected. Most of the lung cancer patients are older than 60 years [3].

Intrafractional motion, in any radiotherapy treatment, will lead to lower target dose coverage and a need for margin enlargement which will increase the dose to the surrounding healthy tissue. One of the challenges in radiotherapy treatment of lung cancer is the difficulty to find the correct cycle path of the tumour which is crucial for the delineation of the PTV. The 4D-CT scanning process has been shown to be a useful tool for localizing the mean position of the tumour and thereby improving the accuracy of the delineation and hence enabling a decrease of the margins. [4] However, healthy tissue will be included in the PTV and increase the risk of complications for the patient.

The need for sparing healthy lung tissue when using radiotherapy has shown to be motivated in many studies see e.g. Hernando et al [5]. This study included 201 patients and showed an increased risk of symptomatic radiation pneumonitis with increasing irradiated volume. The authors looked into dosimetric factors (e.g. volume of lung receiving > 30 Gy, mean lung dose, and normal tissue complication probability derived from models) as well as clinical factors like age, sex, chemotherapy exposure, tumour site, weight loss, smoking habits. It was found that the dosimetric factors were the best predictors of radiation pneumonitis.

One technique to compensate for respiratory movements of the target is respiratory gating. This method is clinically used worldwide for various diagnoses but is most frequently used for breast cancer patients to minimize the radiation dose to the heart. Gated treatments only assert dose delivery when the target is located within a certain position range. [6] When treating moving targets with RapidArc, respiratory gating might be problematic due to the fact that the beam holds will force the gantry rotation to stop. This will compromise the delivery accuracy and increase the treatment time.

Another method to increase the delivery accuracy for moving targets is the DMLC-tracking method. [7] In dynamic MLC (DMLC) tracking the field is reshaped to account for the target motions, and hence the dose delivery is not interrupted. The DMLC-tracking method uses a 3D DMLC tracking algorithm (Varian) with input from a position monitoring system. Studies [7, 8] have been made on the tracking algorithm's capacity to improve conformation of the dose distributions measured with and without moving target. A feasibility study [9] has also been made on DMLC tracking together with RapidArc for a target moving in one dimension with constant speed and peak to peak displacement, showing improved geometric accuracy of the delivery.

The purpose of this study was to evaluate the performance of the DMLC method together with RapidArc^{TM} using dosimetric methods. Special attention was given to its dependence on varying peak to peak displacement and collimator angles.

2. Methods and materials

The DMLC tracking algorithm [10] was tested during RapidArc delivery. Three RapidArc plans were created in Eclipse for a lung tumour case on a patient CT-study. The plans were then calculated for the Delta-4 detector system (Scandidos) [11]. A Real-time Position Management™ (RPM) [12] System (Varian Medical Systems, Inc) was used to monitor the moving target simulated by a motion phantom. The information provided by the monitoring system was used by the MLC controller computer to find the optimal position for the leaves in real-time and to reposition them to best fit the instantaneous location of the target. Measurements were made with peak to peak displacements of the target in the superior-inferior (SI) direction of 5 mm, 10 mm, 15 mm, 20 mm and 25 mm with a cycle time of 6 seconds. The tracking performance when using two different collimator angles of 45º and 90º were evaluated. Measurements were made with the tracking system in three different states: (1) The "disconnected state" where the tracking system is disconnected from the MLC and not affecting the delivery of the plan. (2) The "connected tracking state" where the tracking system uses information about the target location from the RPM system to reposition the MLC leaves. (3) The "connected reference state" where the tracking system is in control of the positioning of the leaves, as in (2) but not receiving information from the RPM system but a zero movement input from a data file. Gamma index evaluation (3% dose difference, 3 mm DTA and 2% dose difference, 2 mm DTA) was used to evaluate the results.

2.1 RapidArc

Varian Medical Systems implementation of the inversely optimized arc radiotherapy technique (RapidArc™) was used for this study. The RapidArc™ technology enables plan delivery in a single or several gantry rotations depending on the version of the treatment planning system used (Eclipse 8.5 or 8.6 and above). During the gantry rotation the MLC, dose rate and gantry speed are changing to create a conformal coverage of the target while sparing the healthy tissue. Varian linacs have a dynamic MultiLeaf Collimator (DMLC) and use the sliding window technique for IMRT delivery. The big advantage of RapidArc is its capacity to deliver a 2 Gy fraction in less than 2 minutes (IMRT ~10 min) without compromising the treatment quality. Another advantage is its ability to deliver a treatment with less monitor units (MU) with IMRT [13]. A recent study has shown that the RapidArc technique is able to perform a treatment with the same target coverage and sparing of organs at risk as IMRT and Helical Tomotherapy™ for treatment of acoustic neurinomas, meningiomas and pituitary adenomas [14]. RapidArc™ technology can be used on the new Varian Trilogy® systems and Clinac® iX linear accelerators and also on other Varian linacs pending a hardware and software upgrade. [13] To reduce the contribution of the tongue-and-groove effect the collimator angle is set to be different than zero (often 45º).

There are currently six clinacs at Rigshospitalet which have RapidArc implemented. All measurements were however performed on the same clinac to reduce inter-

accelerator uncertainties. At the moment, only prostate patients are treated using RapidArc at Rigshospitalet, and these patients are all treated at the same machine.

2.2 Creation of RapidArc plans in Eclipse

CT images of a lung tumour patient case were used to create RapidArc plans for the DMLC tracking measurements. The patient case had a non-small cell lung cancer of state T2N0M0. The target was located in the right lower lobe (fig. 1). The patient case had a previous delineated PTV, lungs and spinal cord. The body outline was determined using a segmentation tool and the heart was delineated manually. The target was defined by creating an inner margin for the original PTV, in the superior-inferior (SI), anterior-posterior (AP) and left-right (LR) direction. The new target was used for the treatment planning optimization process. The size of the original PTV is about 5.8 cm (SI) x 5.4 cm (AP) x 4.7 cm (LR) (volume of 70.40 cm^3) and the size of the new target is about 3.1 cm (SI) x 3.6 cm (AP) x 3.1 cm (LR) (volume of 12.42 cm^3).The reason for creating a smaller target than the original PTV was the aim to create a small field opening to keep the penumbra within the high resolution area of the detector arrays during the measurements. The resolution is high (0.5 cm) in a region of 6 cm x 6 cm at the centre of the detector area and 1 cm at the rest of the detector area. The tumour was situated almost in the centre of the right lung (figure 1) and the GTV volume was 24.39 cm^3. Three treatment plans were created in Eclipse™ (Aria ver. 8.5). The plans were created using identical settings apart from the collimator angle that was set to 45º for two of the plans and 90º for one plan. The plan parameters are shown in table 1.

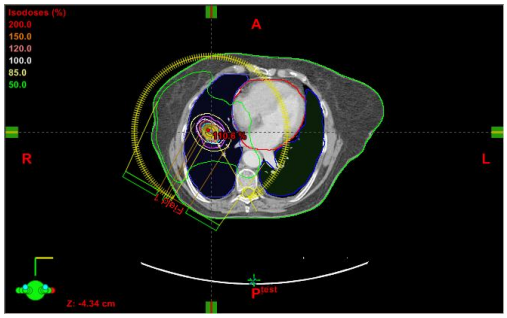

Figure 1 Isodoses for Plan 1(45) in Eclipse™

Table 1 Plan parameters

Machine	Clinac 12
Energy	6 MV (photons)
Dose/fraction	2 Gy
Collimator angle	45º or 90º
Gantry angles	210º - 150º

The collimator angle of about 45º is the most commonly used for RapidArc since it enables creation of more complicated field shapes than with a non-rotated collimator. DMLC tracking has shown to have the best performance for tracking targets moving in parallel with the leaf trajectory. [7] This enables the MLC to compensate for the target displacements by moving the leaf pairs that are already opened and not changing the position of the closed leaves adjacent to the field opening. This gives a more dynamic adjustment of the field shape compared to the discrete steps (of the size of the leaf width) that are unavoidable when the target is not moving in parallel with the leaf trajectory. In this study the movement of the target was in the SI direction and the collimator was thus set to 90º to enable tracking parallel to this motion. This angle is not favourable for RapidArc delivery

due to the dose distribution arising from the leakage between the closed leaf tips and the rotational dose delivery. A small deviation from the 90 degree collimator angel would decrease the leakage and tongue-and-groove effects and there are no restrictions on what collimator angle that can be used for MLC tracking. However, a small difference in collimator angle from the parallel settings might result in closed leaf pairs being opened, and to ensure that this would not happened during the experiments, the collimator angle of 90 degrees was chosen. A collimator angle of 90 degrees is not clinically relevant for RapidArc treatments and was used only to test the performance of the system for MLC settings that has been shown to be preferable for tracking [7].

The gantry angles were limited to run from 210º to 150º to prevent the beam from entering through the rails of the couch. To start the optimization process, dose volume objectives were defined according to the standards at the hospital. Priorities for the dose distributions were assigned to grade their importance to match the objectives, with the more crucial objectives given the highest priority (4) and the less crucial objectives given a lower priority (1) (table 2 and 3).

Table 2 Dose-volume objectives for target

Target	Volume [%]	Dose [Gy]	Priority
Upper limit	0	62	2
Lower limit	100	58	4

Table 3 Dose-volume objectives for OAR:s (approximate values)

Organ at risk	Upper limit volume [%]	Upper limit Dose [Gy]	Priority
Heart	50	30	1
	30	45	1
	20	50	1
	0	60	1
Lungs	20	20	1
Spinal cord	10	45	1
	0	50	2
Body	0	62	2

The Normal tissue (total CT volume excluding the target) objectives as a function of the distance from the target border are alterable but were in these cases kept as the predefined values (by Varian) and are shown in figure 2 and table 4.

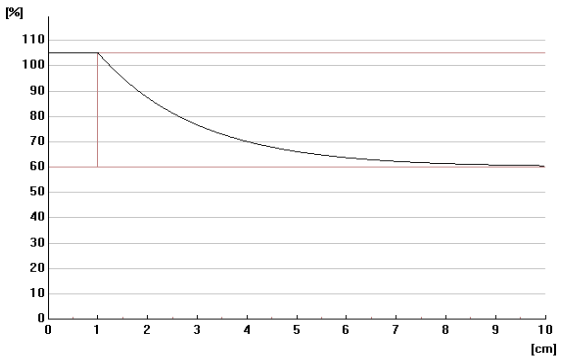

Figure 2 Normal tissue objective for the RapidArc plans

Table 4 Normal tissue objective for the RapidArc plans

Distance from target border [cm]	1
Start dose [%]	105
End dose [%]	60
Fall-off	0.05

2.2.1 Optimization process

The principles of the optimization process that are used by the treatment planning system (TPS) are described in detail by Otto [2], but are summarized here for clarity.

The Progressive resolution optimisation (PRO) algorithm, starts off with ten control points (CPs) evenly distributed over the gantry arc, and the first resolution phase has a distribution of MLC shapes with the maximum allowed gantry speed and dose rate. The MLC shapes, gantry speed and dose rate are then optimized in 5 multiresolution levels with a fixed number of iterations and in the end of each multiresolution level the number of CP: s is increased with a factor of 2. The process ends when the number of CP: s reaches 177. During the optimization process, variations of MLC shapes, dose rates and gantry speeds are tested simultaneously to find the plan that best fulfils the dose volume objectives defined by the user. An intrinsic stochastic component is added in the process to avoid traps in local minima. This will give the effect that two optimizations for the same dose volume objectives and CT data will give two different RapidArc plans. When the dose per degree needs to be adjusted, the dose rate is modified and the gantry speed is kept as high as possible. The gantry speed is decreased only when the dose rate has reached its maximum allowed value without being able to deliver the desired dose/degree, thus keeping the treatment time as short as possible. [2]

2.2.2 Dose calculation

After the optimization process the volume dose was calculated using the Anisotropic Analythical Algorithm (AAA) with a calculation grid size of 0.25 cm. The monitor units (MUs) for the RapidArc plans are shown in table 5.

Table 5 Number of monitor units for the RapidArc plans

Plan	Collimator angle	Number of MU:s
1(45)	45º	379
2(45)	45º	367
3(90)	90º	410

The differences between plan 1(45) and 2(45) are due to the fact that they were created during different runs of the optimization process. The DVH of plan 1(45) (fig. 3) shows a rather poor coverage of the target compared to what is normally seen in a conventional CRT or IMRT plan based on the Pencil Beam calculation model. This is because the plan is calculated using the AAA instead of the more commonly used Pencil Beam (PCB) model.

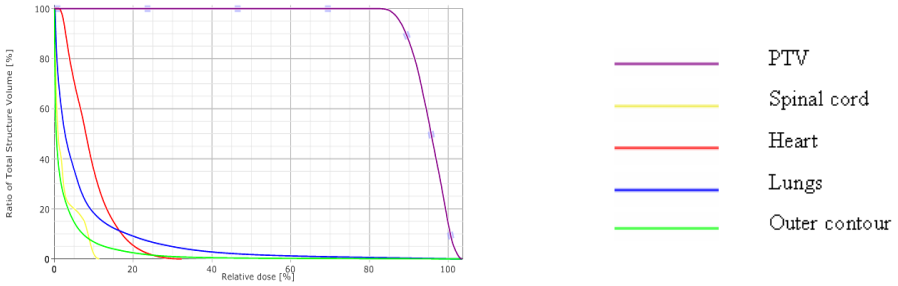

Figure 3 The DVH of RapidArc plan 1(45)

The main difference between the AAA calculation model and the PCB model is the way of handling the density variations in the volume. The PCB model does not correct the kernel for lateral density variations. [15] This will cause a problem when calculating dose distributions in a heterogeneous volume (for example a small lung tumour). The AAA algorithm on the other hand has the lateral extension of the pencil beam scaled with the densities relative to water. [15] The lateral description of the pencil beam is divided into three terms; one for the produced electrons and two for the scattered photons. This makes the dose calculation more accurate when considering a small tumour in a volume with very low density, like in the CT-data in this case. [15] The AAA is thus a better choice for the dose calculations in this case but it was also the only available calculation model for RapidArc plans in Eclipse.

The RapidArc plans were transferred to the Delta-4 dosimetric system as verification plans. To enable tracking parallel with the MLC leaf trajectory, the carriages were pushed to the sides by manually setting the 1A and 1B leaves (i.e. the leaves at the ends of the leaf rows) to 7 cm. The editing was done in the TPS system before importing the plan on the 4DTC treatment consol. The MLC plans were exported from the non-edited RapidArc plans to obtain the planned leaf positions at the tracking computer. However when exporting the MLC plan, the gantry angle information was lost and had to be restored before use. A program was created for this purpose using MATLAB (Mathworks, Natick, MA).

2.3 Measurements

The measurements were made at Rigshospitalet using a clinically installed Varian 2300ix Clinac with RapidArc capabilities. Measurements were made in the following states of the tracking system with moving and static target:

The disconnected state (1) is when the tracking controller has no connection to the MLC and does not affect the delivery of the plan. Measurements were made with a moving target in this state to use in comparison with the measurements where the tracking method was used. When evaluating these results, gamma index evaluation was made using a static target measurement in the same state as the reference. The pass rate is an indication of how much the dose distribution has changed due to the movement of the target.

The connected tracking state (2) is when the tracking system controls the positioning of the MLC leaves and uses information about the target location from the RPM system to reposition them in real-time. Measurements were made with a moving target in this state to evaluate the DMLC tracking methods ability to compensate for target movements. When evaluating these results, gamma index evaluation was made using a measurement of a static target in the connected reference state (3) as the reference. The connected reference state was used as a reference to avoid the difference in the dose distributions due to leakage from the adjacent leaf pairs. This was done to give a fair value of the change in dose distribution due to the target movements when using tracking, not the difference in leakage due to different positioning of the adjacent leaf pairs (see “Plan preparation for DMLC tracking, page 12).

The connected reference state (3) is when the tracking system controls the positioning of the MLC leaves but receives information about the target positioning from a data file, not the RPM system. The data file contains information about a static target and the detector is kept static for the measurements in this state. Therefore, the measurements in this state do not contain any noise from the RPM system but has the adjacent leaf pairs moved to the side as in the connected tracking state (see "Plan preparation for DMLC tracking, page 12).

2.3.1 MLC controller software

The DMLC-tracking algorithm was created by Varian medical systems [10] and the MLC tracking research group at Stanford University [16]. The software is a non-clinical research tool and the development of the tracking code is presently on-going. The principles of the DMLC tracking method is to reposition the MLC leaves according to the displacement of the target to create an optimal field shape taking the target shape and position into account.[7] In RapidArc plans the MLC leaf positions are defined as a function of control points (with linear relation to the gantry angle except for the first and last control points), in contrast to IMRT plans where the MLC positions are defined as a function of MUs. The MLC sequences of the RapidArc plans that were to be measured were exported from the TPS to the tracking computer. When the tracking system is connected, the MLC controller will be in control of the positioning of the leaves using the information from the MLC sequence to find the planned position of the leaves for every control point. The tracking computer was connected to the treatment consol via the local network. The tracking controller computer receives real-time information about target location from a position monitoring device through a serial port connection. This information was transformed from room coordinates to a coordinate system corresponding to the beam's eye view using the tracking algorithm. [7] The tracking algorithm calculates the new leaf positions in beam's eye view coordinates, by determining the intersection between each leaf trajectory and the planned field outline repositioned according to the information from the position monitoring device. The midpoint of the outer edge of each leaf goes to the closest point of intersection. The finite width of the MLC leaves is a limiting factor of the accuracy of the method, but by introducing a number of small, virtual sub-leaves for every MLC leaf, the accuracy can be improved. [7] The tracking code contains a prediction algorithm to compensate for temporal latencies due to the time consumption of detecting target motion, for calculating the new leaf positions and the time for the MLC leaves to move (~160 ms when using the RPM system). This was not used for this work since problems during the development of this part of the tracking code made it unfavourable to use. It has been shown that reduction of the response time will increase the over-all system accuracy.[8] It can therefore be assumed that the results of this study would be improved if a functioning prediction algorithm was used. DMLC-tracking of sinusoidal motion using a prediction algorithm should not be challenging due to the periodic nature of the motion. When the DMLC tracking algorithm is used for IMRT or conventional RT, beam holds are asserted in case of anomalous situations, such as target moving underneath one of the jaws or too quickly for the leaves to keep up, in order to ensure optimal delivery. However, when using MLC-tracking in IMAT or RapidArc delivery, it has been chosen not to assert beam holds because interruptions in the arc delivery

(and rotation) is considered to have a worse impact on the treatment than tracking related issues.[15]

2.3.2 Plan preparation for DMLC tracking

The jaws were positioned sufficiently far enough apart to allow tracking for the largest conceivable peak to peak displacements of the target. For this study, the jaw positioning was set to 13 cm x 13 cm. This was done after the optimization process of the RapidArc plans. The artificial placement of the jaws results in exposing several closed leaf pairs. Therefore, when the MLC leaves are not participating in field shaping, they are pushed under the jaws by the tracking system to reduce radiation leakage between the small gap of a closed leaf pair. Exception was taken for the three leaves closest to the field opening. These were kept at the centre and ready to be opened if the target was to move in their direction. When performing the measurements presented in this work, there was a bug in the tracking code that resulted in one of the sides of the opened field only having two adjacent leaf pairs kept at the centre. This was discovered after the last measurements were performed.

Another important preparation step was the settings of the MLC carriages. These need to be pushed to the side to allow tracking in the direction parallel to the leaf trajectory. This was done by setting the 1A and 1B leaves to 7 cm in the TPS after the optimization process. Only the first field that was opened on the 4DTC needed to be edited for this purpose since the carriage does not move during the delivery. To avoid MLC interlocks (because of limitations in the velocity of the MLC leaves) the opening of the 1A and 1B leaves were gradually decreased by 0.5 cm every following control point until they reached the closed position.

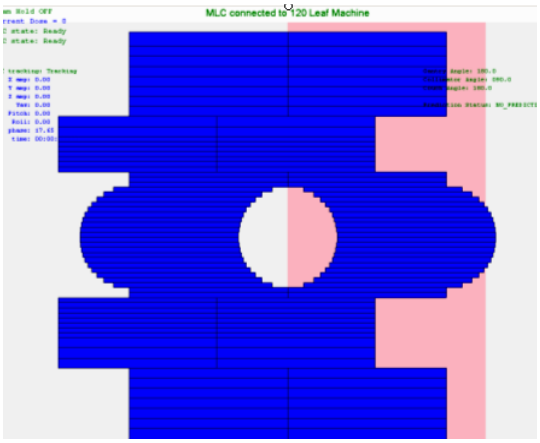

Figure 4 MLC leaf positions in the connected tracking state and the connected reference state

2.3.3 Simulation of target movements

Studies on 3D tumour motion in the lung due to breathing and heart beat has shown that the motion mainly occurs in the SI direction. [17] The same study presents patient cases with 0.2-25 mm peak to peak distance for movements in the SI direction and cycle times of 2.7-6.6 seconds. Based on this data and the limitations of the motion phantom that was used, the displacement lengths were chosen to be 5 mm, 10 mm, 15 mm, 20 mm and 25 mm and the cycle time was chosen to be 6 seconds for all measurements. A long cycle time was desirable since no prediction algorithm was used.

2.3.3.1 Respiratory gating platform

The target movements were simulated by a 1D Respiratory gating platform (Standard Imaging) [18] (fig. 5) with adjustable displacement lengths and cycle times. The technical specifications of the Respiratory gating platform are listed in Appendix III. The gating platform was not CT-scanned together with the dosimetric

systems but was added manually to the verification plans before the dose calculation. The Hounsfield unit of the platform was found by making separate measurements using a solid water phantom with an ion chamber on 5 cm depth. The phantom was irradiated with 100 MU, the dose rate was 600 MU/min, the field size was 10x10 cm and the SSD was 95 cm. The measurements were performed with and without the platform on top and the transmission were approximated by forming the ratio of the charge collection by the electrometer. A structure with the same dimensions as the platform was created manually in the TPS in a plan with a similar solid water phantom as the one in the measurements. The dose was then calculated for the measured point of the plan and for an equivalent plan without the platform and the quotient was derived. New plans with different CT-values for platform were then created until the measured and calculated quotiens were consistent (HU=108). The CT-value was in the range of values measured in an earlier scan of the same platform (HU = 70 -160). The Respiratory gating platform was mounted on the treatment couch (fig. 9) to carry the detector system. The accuracy of the cycle time of the Respiratory gating platform was tested by measuring the time of ten cycles and calculating the average time for one cycle. The accuracy of the displacement lengths were tested by manually displacing the movable part of the platform to its outer positions for the peak to peak displacements used. The distance between these positions were then measured with a ruler.

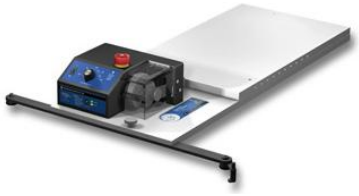

Figure 5 Respiratory gating platform [18]

2.3.4 RPM position monitoring device

The tracking computer received information about the 3D localization of the phantom from a Varian® Real-time Position Management™ (RPM) system. The information was used by the tracking controller to correct the planned MLC positions according to the target movements. The RPM system is presently used in the clinic for gated treatments where the radiation dose is delivered only when the target is located within a certain position range. The system can be used when treating lung, liver and pancreas, but is most frequently used for breast cancer patients to reduce the dose to the heart. The system uses an infrared camera and a marker block with reflective markers to estimate the target position relative to the calibration point.[12] To monitor 3D movements, the 6-marker block (fig. 6) was used and the RPM software was set not to use temporal averaging (normally used in clinical gating monitoring) to reduce the latency of the system. The marker block was placed on the dosimetric device (fig. 8) to measure its displacement in the SI direction.

Figure 6 RPM (Varian) [24]

A shift of the dose profiles was noted for some of the measurements and appeared to be related to instabilities in the RPM system. Since the target had a convex shape and the target dose was fairly homogenous, this shift could be quantified as:

$$Shift = \left(x_{1(ref)} + \frac{FWHM_{ref}}{2} \right) - \left(x_1 + \frac{FWHM}{2} \right) \quad (1)$$

$$FWHM = x_2 - x_1 \quad (2)$$

Where x_1 and x_2 are the positions in the SI direction receiving half the maximum dose. These points were found by interpolating (linearly) between the two closest detectors.

The shift of the profiles of the performed measurements in the connected tracking state was in the range of 0.01 mm to 4.25 mm (see section 3.4).

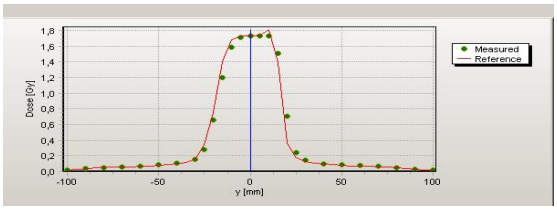

Figure 7 Example of profile shift. The red line is the reference measurement and the greed dots is the measurement with a moving target

Separate measurements were made to investigate the RPM system's influence on the tracking performance to evaluate if there were instabilities in this system that could have created the profile shifts.

The influence of the RPM system on the tracking performance for a static target was investigated using static target measurements in the connected tracking state and in the connected reference state. Gamma index evaluation was then used to evaluate the results using a static target measurement in the disconnected state as reference.

The RPM systems stability over time was investigated by acquiring position information of a static marker block for 20 minutes. The experiment was then repeated without calibrating the system in between. To check the reproducibility of the experiment, the system was then calibrated and the experiment was performed another two times. Linear regression was used to estimate the RPM drift over time.

The noise level of the RPM system was investigated by calculating the standard deviation for the 20 min static acquisitions described above.

The RPM system's ability to estimate the correct position of the marker block when it is moved during the acquisition was investigated using four 1-hour measurements with the RPM system. The marker block was repositioned 30 times for every measurement at 0 cm, +1 cm and -1 cm from the calibration position for two of the measurements and 0 cm, +2 cm, -2 cm for the other two measurements. A ruler (0.5 mm steps) was used to verify the marker block position.

The RPM system was recalibrated before every measurement in the connected tracking state since this appeared to reduce the shift of the profiles.

2.3.5 Dosimetric system

The Delta-4 dosimetric (ScandiDos) [11] system (fig. 8) was used for the measurements in this study. The system enables dose measurements isotropicly over 360º rotation and it has the possibility to reconstruct the delivered dose in 3D. Each accelerator pulse is measured separately. The phantom contains two crossing

orthogonal planes of p-Si diodes surrounded by PMMA shaped as a cylinder. The spatial resolution of the detector system is 0.5 cm at the centre of the detector planes (6 cm x 6 cm) and the rest of the detector area has a spatial resolution of 1 cm. [11] The technical specifications for the ScandiDos Delta-4 are listed in Appendix III. The detector system was mounted on the respiratory gating platform (fig. 9).

Figure 8 ScandiDos Delta4 [11]

The Delta-4 evaluation software has a tool for visual comparison of dose profiles. The user can study profiles in the two dimensions of the detector arrays. To visualize the impact of the target movement on the dose distribution, and the change in dose profiles when the tracking system is connected, profiles in the SI direction of one of the arrays were visually analyzed.

Figure 9 Experimental setup. The Delta-4 was mounted on the Respiratory gating plaform on the treatment couch. The RPM marker block was positioned on top of the Delta-4.

2.4 Evaluation

The Delta4 software contains evaluation tools for comparison of dose distributions. The evaluation tools available in the Delta4 software are the dose deviation evaluation method, the distance to agreement evaluation method and gamma index evaluation method.

The dose deviation evaluation method compares the dose in the data points that is to be evaluated, with the corresponding points in the reference data.[19] A criteria for the maximum allowed dose deviation is chosen by the user (often 3 %). In the delta4 evaluation software the criteria is set with respect to the global dose. In this study, the isocenter dose was used. The dose threshold was set at 10% to 500% to include the penumbra but not the peripheral detectors which were considered not to be affected by the tracking method. To pass the dose deviation evaluation, the dose

in the data point to be evaluated cannot deviate more than this selected percentage from the reference data.

The distance to agreement (DTA) method considers the distance between the point to be evaluated and the nearest data point in the reference data with the same dose. [19] The Delta 4 interpolates between the data points in the reference data set to create an isodose surface to compare with the data points that are to be evaluated. However, it only considers a maximum distance of 20 mm. If the distance to the closest point with the same dose is larger than 20 mm, the DTA is set to be 20 mm. A criteria for the maximum allowed DTA is chosen by the user (often 3 mm). To pass the evaluation, the distance between the data point to be evaluated and a point in the reference data with the same dose can not exceed this value. The dose deviation evaluation method is suitable to use in regions with low dose gradients since a point with a small dose deviation would fail the DTA evaluation in this region. The DTA evaluation method on the other hand is suitable for evaluation in regions with high dose gradients since the dose deviation evaluation method would fail the evaluation for data points with the same dose but with a very small spatial difference.

The gamma index evaluation method combines the two methods described above, setting criteria for both the dose deviation and the distance to the nearest data point with the same dose in the reference data. [19] This method can be used in regions with both high and low dose gradients. Low et al [19] describes how to calculate the gamma index:

$$\Gamma(r_m, r_c) = \sqrt{\frac{r^2(r_m, r_c)}{\Delta d^2{}_M} + \frac{\delta^2(r_m, r_c)}{\Delta D^2{}_M}} \tag{3}$$

Where

r_m is the data point to be evaluated

r_c is the corresponding data point in the reference data

$r(r_m, r_c)$ is the distance from the data point to be evaluated a point in the reference data with the same dose

Δd_M is the DTA criteria

$\delta(r_m, r_c)$ is the dose deviation between the data point to be evaluated to the corresponding point in the reference data

ΔD_M is the dose deviation criteria

The gamma index value is the smallest possible value for eq. (1) for all data points in the reference data:

$$\gamma(r_m) = \min\{\Gamma(r_m, r_c)\} \forall \{r_c\} \tag{4}$$

If the gamma index is smaller or equal to one, the data point passes the evaluation:

$\gamma(r_m) \leq 1$ calculation passes

$\gamma(r_m) > 1$ calculation fails

For this study the gamma index was primarily used for the evaluation, but attention was also given to the other methods. The criteria used in this study were 3 % and 3 mm, and 2% and 2 mm.

Since the purpose of this study was to investigate the tracking controller performance and not the characteristics of the RPM system, measurements where the shift was regarded to have a big impact on the result was not included in the evaluation. When using criteria of 1%, 1mm for the gamma evaluation, the majority of the measured data were greatly affected by the profile shift (see section 3.4). The percentage of points that passed the gamma index evaluation showed a strong linear dependence on the profile shift. The criteria 1%, 1mm was therefore not used to evaluate the results. When using criteria of 2%, 2mm for the gamma evaluation, the majority of the measurements did not show a dependence on the profile shift and these criteria were therefore used to evaluate the results. The data that were seen to have been affected by the profile shift for these criteria (profile shift > 1.3 mm) was not included in the evaluation.

2.5 Calculation of DMLC tracking's ability to facilitate margin reduction

The PTV margin is created to account for treatment execution and treatment preparation variations. Execution variations, such as variations in set up and tumour location during the treatment, are random and will lead to a blurring of the dose distribution. Preparation variations, such as uncertainties in the CT-scanning process and the delineation of the tumour, will systematically affect all treatment fractions the same way and lead to a shifted dose distribution. To evaluate how the DMLC tracking method can affect the choice of margin size, one first has to consider how the dose smearing depending on the target movement is accounted for in the margin size. van Herk et al [20] present a method for creating PTV margins that accounts for both systematic and random errors. The method is briefly summarized bellow.

The total PTV margin is given by:

$$m_{ptv} = \alpha\Sigma + \beta\sigma - \beta\sigma_{penumbra} \tag{5}$$

where

Σ is the combined standard deviation of all preparation errors
α = 2.5 for 90% confidence interval in 3D
β = 1.64 for the 95 % isodose surface

σ is the total SD for all random variations and can be calculated as

$$\sigma^2 = \sigma_{motion}^{\ 2} + \sigma_{setup}^{\ 2} + \sigma_{penumbra}^{\ 2} \tag{6}$$

The SD of variations due to the target motion and set up of the patient are represented by σ_{motion} and σ_{setup} and the SD describing the penumbra width is denoted $\sigma_{penumbra}$.

$\beta\sigma_{penumbra}$ is equal to the distance between the 95% and 50% isodose surface of the planned dose distribution and $\beta\sigma$ is equal to the distance between the 95% and 50% isodose surface of the dose distribution affected by the random variations. The margin that is needed to account for execution variations can be calculated as the difference between these two values

$$\beta\sigma - \beta\sigma_{penumbra} \tag{7}$$

The 50% isodose surface can be used as reference since this does not change in position due to random variations.

To estimate the profit of using DMLC tracking during RapidArc delivery to a moving lung tumour, the difference in the required PTV margin for delivery with and without the use of the DMLC tracking method was calculated as

$$m_{PTV,Disconnected\ state,lung} - m_{PTV,Connected\ tracking\ state,lung} \tag{8}$$

$$= \left(\alpha\Sigma + \beta\sigma - \beta\sigma_{penumbra}\right)_{Disconnected\ state,lung} - \left(\alpha\Sigma + \beta\sigma - \beta\sigma_{penumbra}\right)_{Connected\ tracking\ state,lung} \tag{9}$$

$$= \beta\sigma_{Disconnected\ state,lung} - \beta\sigma_{Connected\ tracking\ state,lung} \tag{10}$$

$$= \beta\left(\sqrt{\sigma_{motion,DS,lung}^{\ 2} + \sigma_{set\ up,lung}^{\ 2} + \sigma_{penumbra,lung}^{\ 2}} - \sqrt{\sigma_{motion,CTS,lung}^{\ 2} + \sigma_{set\ up,lung}^{\ 2} + \sigma_{penumbra,lung}^{\ 2}}\right) \tag{11}$$

The SD describing the width of the penumbra in the lung, $\sigma_{penumbra,lung}$, was found by measuring the $\beta\sigma_{penumbra}$ for four RapidArc plans in the TPS. The average value was calculated and divided by β. The SD for the set up of the patient, $\sigma_{set\ up,lung}$, was approximated to 5.3 mm in the SI direction [21]. The SD for the target motion when using the disconnected state, $\sigma_{motion,DS}$, and the connected tracking state, $\sigma_{motion,CTS}$, were found by calculating the average $\beta\sigma$ for the measurements with a moving target in the different states of the tracking system for plan 1(45). The difference in margin size needed for the different states of the tracking system was calculated for the superior and inferior side of the tumour for the motion amplitudes studied in this work. Dose information from detectors along the central line in the SI direction of one of the detector arrays of the Delta4 was used to calculate $\beta\sigma$. The value of σ_{motion} could then be calculated as

$$\beta\sigma_{DS,D4} = \beta\left(\sqrt{\sigma_{motion,DS}^{\ 2} + \sigma_{set\ up,D4}^{\ 2} + \sigma_{penumbra,D4}^{\ 2}}\right) \Leftrightarrow \sigma_{motion,DS}^{\ 2} = -\left(-\left(\frac{\beta\sigma_{DS,D4}}{\beta}\right)^2 + \sigma_{set\ up,D4}^{\ 2} + \sigma_{penumbra,D4}^{\ 2}\right) \tag{12}$$

$$\beta\sigma_{CTS,D4} = \beta\left(\sqrt{\sigma_{motion,CTS}^{\ 2} + \sigma_{set\ up,D4}^{\ 2} + \sigma_{penumbra,D4}^{\ 2}}\right) \Leftrightarrow \sigma_{motion,CTS}^{\ 2} = -\left(-\left(\frac{\beta\sigma_{CTS,D4}}{\beta}\right)^2 + \sigma_{set\ up,D4}^{\ 2} + \sigma_{penumbra,D4}^{\ 2}\right) \tag{13}$$

The standard deviation for the variations in set up and the width of the penumbra for the Delta-4 measurements, $\sigma_{set\ up,D4}$ and $\sigma_{penumbra,D4}$ were found by calculating the $\beta\sigma$ for static measurements in the connected tracking state for plan 1(45)

$$\beta\sigma_{Static,DS,D4} = \beta\sqrt{\sigma_{set\ up,D4}{}^2 + \sigma_{penumbra,D4}{}^2} \Leftrightarrow \sigma_{set\ up}{}^2 + \sigma_{penumbra,D4}{}^2 = \left(\frac{\beta\sigma_{static,DS,D4}}{\beta}\right)^2 \quad (14)$$

The possible reduction of the PTV margin can then be calculated as

$$m_{PTV,Disconnected\ state,lung} - m_{PTV,Connected\ tracking\ state,lung} \quad (8)$$

$$= \beta\left(\sqrt{-\left(-\left(\frac{\beta\sigma_{DS,D4}}{\beta}\right)+\left(\frac{\beta\sigma_{static,DS,D4}}{\beta}\right)^2\right)+\sigma_{penumbra,lung}{}^2+\sigma_{set\ up,lung}{}^2} - \sqrt{-\left(-\left(\frac{\beta\sigma_{CTS,D4}}{\beta}\right)+\left(\frac{\beta\sigma_{static,DS,D4}}{\beta}\right)^2\right)+\sigma_{penumbra,lung}{}^2+\sigma_{set\ up,lung}{}^2}\right) \quad (15)$$

3. Results and Discussion

3.1 Results of the gamma evaluation

The results of the gamma evaluation are shown in fig. 10-11. The mean of the percentage of points passing the gamma index evaluation is calculated using 1 to 6 measured values (see Appendix I for the number of measured values for each plan and peak to peak displacement) and plotted against the peak to peak displacement. The error bars indicate one standard deviation of the measured values. Detailed results of the gamma index evaluations, dose deviation evaluations and distance to agreement evaluations are given in Appendix I. The results of the gamma index evaluation for 2% 2 mm show a significant increase in delivery accuracy for the measurements in the connected tracking state to the measurements in the disconnected state. There is a weak trend that the 90º collimator angle is a superior angle for tracking than 45º. The somewhat better results of plan 2(45) compared with plan 1(45) should not be considered as a difference in the tracking performance since the statistics of plan 2(45) is too low to support this conclusion. Plan 1(45) and 2(45) are very similar plans with 379 MU and 367 MU respectively.

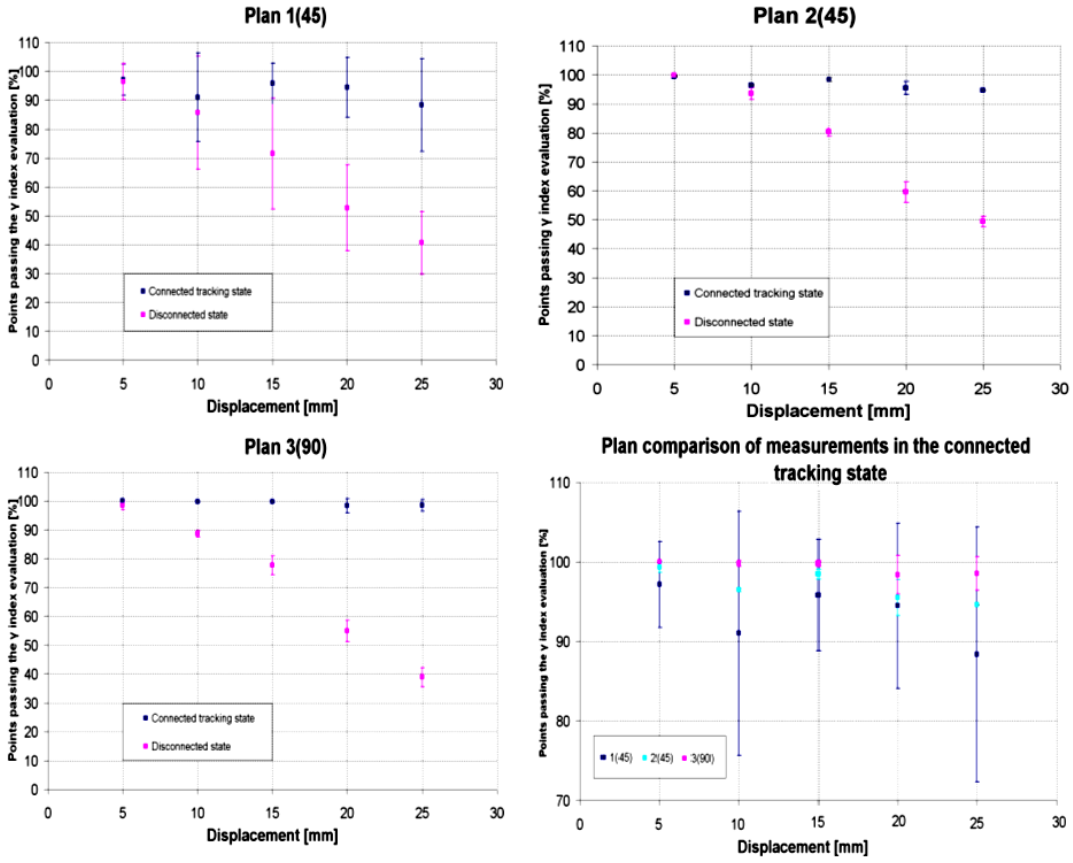

Figure 10a.-d. Gamma index evaluation with criteria 2%, 2mm. The measurements made on a moving target in the disconnected state are evaluated with static target measurements in the same state as reference. The measurements made on a moving target in the connected tracking state are evaluated with a static target measurement in the connected reference state as reference

The gamma evaluation with criteria 3%, 3mm shows the same trend as the evaluation with the 2%, 2mm criteria. For these criteria, the pass rate for the evaluated data points is higher for both states, giving a larger effect on the measured data in the disconnected sate. The data points received in the connected tracking state measurements are close to 100%. The gamma evaluation with criteria 3%, 3mm also shows a small trend that the 90º collimator angle is a superior angle for tracking compared with 45º.

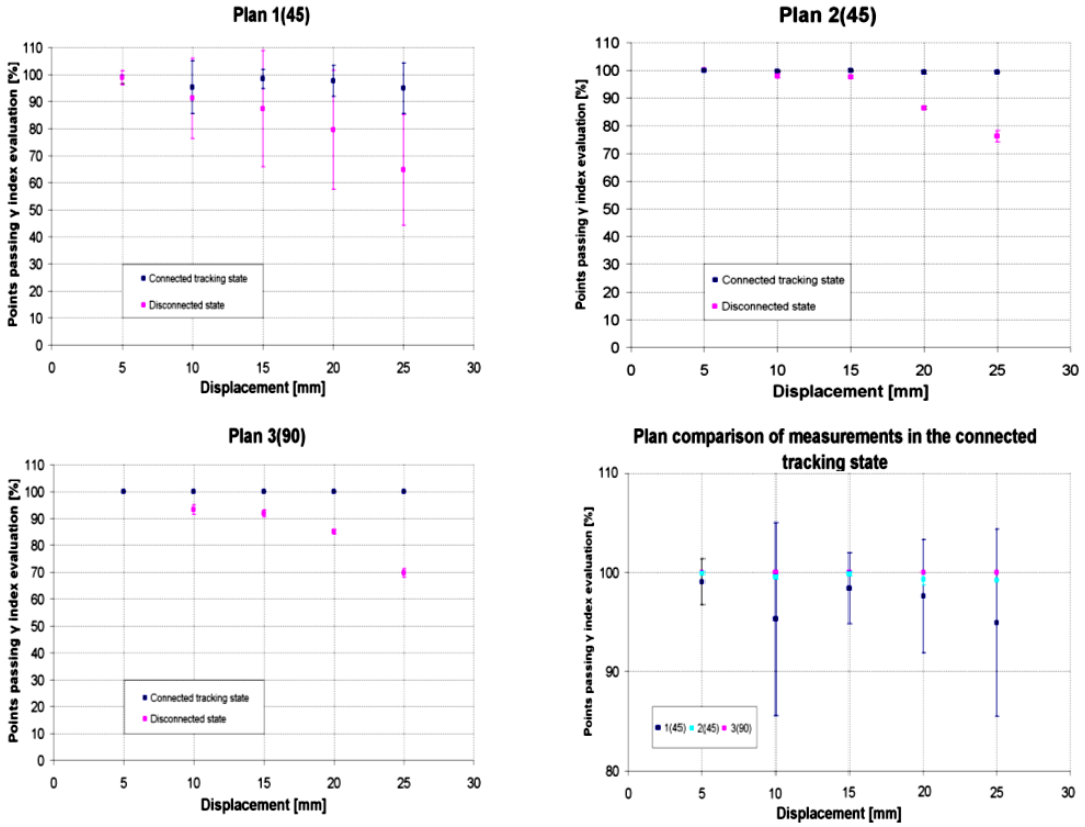

Figure 11a.-d. Gamma index evaluation with criteria 3%, 3mm. The measurements made on a moving target in the disconnected state are evaluated with a static target measurement in the same state as reference. The measurements made on a moving target in the connected tracking state are evaluated with a static target measurement in the connected reference state as reference

All calculated means of pass rate in the gamma index evaluations are based on one to six measured values. The statistical uncertainties are therefore not sufficiently small to draw any conclusions about variations in the tracking performance depending on collimator angle or variations of individual plans. The results did not show a decrease in tracking performance depending on the size of the peak to peak displacement of the target. The variations in the average value of the gamma index pass rate for the different displacement sizes are within one standard deviation of the measurements.

3.2 Evaluation of dose profiles

The results of the visual evaluation of the dose profiles showed a clear reduction of the dose smearing for the measurements in the connected tracking state. An

example of this evaluation is shown in fig.12. The measurement with a moving target is shown as green dots and the reference measurement is shown as a red line. The profiles measured in the disconnected state show an increase in "dose-smearing" as the peak to peak displacement increases. The profiles measured in the connected tracking state show a superior conformation to the reference measurement. Note that the reference measurements for the different tracking system states are not the same (see section 2.3).

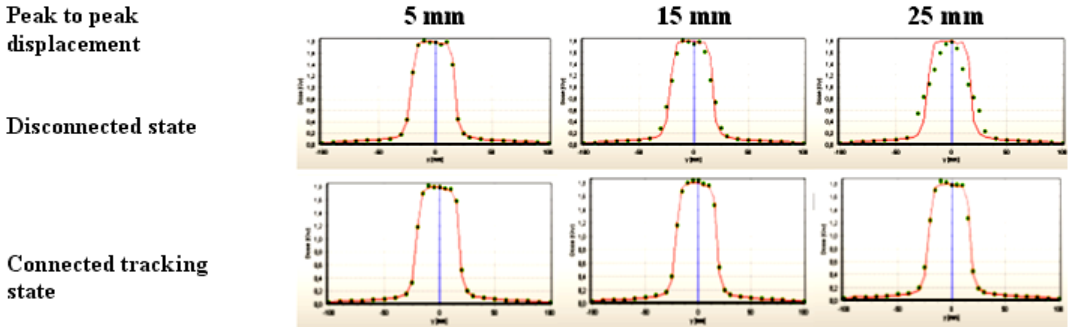

Figure 12 Dose profiles in the SI direction of measurements in the disconnected state (top) and the connected tracking state (bottom). The red line shows the profile of the same detectors but for the reference measurement. Profiles are shown for 5 mm, 15 mm and 25 mm displacement of the target.

3.3 DMLC tracking's ability to facilitate margin reduction

The results of the calculation of the possible margin reduction when using DMLC tracking are shown in table 6 and in fig.13. The values of $\sigma_{penumbralung}$ were calculated to 8.2 mm (cranial side) and 14.7 mm (caudal side). The result suggests that DMLC tracking possibly can enable margin reduction for large motion amplitudes.

Table 6 Results of the calculation of the possible margin reduction when using DMLC tracking

Peak to peak displacement [mm]	Margin reduction on the cranial side of the target [mm]	SD	Margin reduction on the caudal side of the target [mm]	SD	Number of values for σ_{motion} used in the evaluation
5	0.1	0.08	-0.04	0.11	6
10	1.63	0.72	0.62	0.66	5
15	2.62	0.42	1.63	0.33	5
20	3.7	0.28	2.03	0.28	6
25	5.29	1.12	3.54	1.13	4

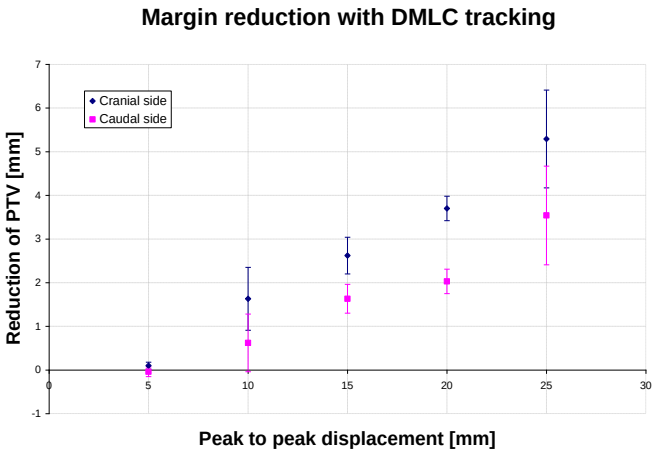

Figure 13 Calculated reduction of margins when using the DMLC tracking method

At the moment, the PTV margin for lung tumours is usually not individualized at Rigshospitalet. The same margin size is used for most patients and hence not individualized and dependent on tumour motion in a specific patient. However, in cases where there is a strong need for reduction of the dose to healthy lung tissue, the margin may be reduced.

3.4. Investigation of the influences of the RPM system

3.4.1 Dose profile shift

The shift of the dose profiles were calculated for all measurements. The results are shown in fig. 14-15. There is a strong dependence of the gamma index pass ratio on the profile shift for the 1%, 1 mm criteria, which is not surprising since the profile shift for most of the measurements are of the same magnitude or larger than the criteria for DTA (fig. 14). For this reason, the 1%, 1 mm criteria was not used when evaluating the results. To avoid the results being affected by the profile shift for the other criteria, the measured data points with a profile shift larger than 1.3 mm (the value of the smallest shift in fig. 15 where the linear dependence between the gamma index (2%, 2 mm) pass ratio and the profile shift is apparent) were excluded from the evaluations.

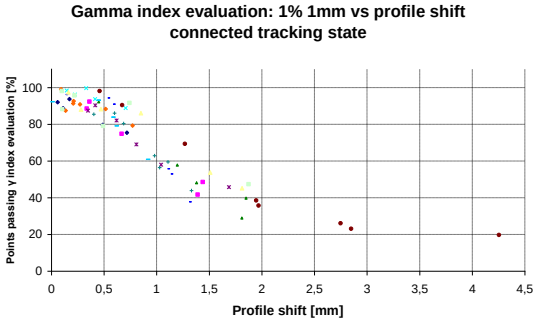

Figure 14 Profile shift of the measured data

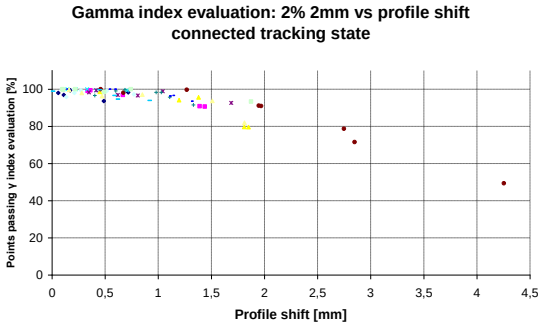

Figure 15 Profile shift of the measured data

3.4.2 The RPM system's influence on the tracking performance

The static measurements in the connected tracking state and connected reference state was evaluated using gamma index evaluation (3%, 3mm and 2%, 2mm) with a static target measurement in the disconnected state as reference. The results of this evaluation are shown in fig.16. There is a trend that connected tracking state has better agreement with the disconnected state than the connected reference state has. However, for plans 1 and 3, there is no significant difference between the connected states, since the deviation is within one standard deviation. If the RPM system would have a worsening effect on the performance of the tracking system when tracking a static target, the connected reference state would have a higher pass rate than the connected tracking state in the gamma index evaluation. The difference in pass rates between the plans is most likely due to difference in the distribution of the leakage dose from the closed leaves. The 90º collimator angle of plan 3 concentrates the leakage dose to a smaller volume, which will give a relatively large dose deviation in a small volume. The leakage dose of plans 1 and 2 (45º collimator angle) were distributed over a larger volume which results in a smaller dose deviation in a larger volume. This results in plan 3(90) having a lower pass rate for gamma criteria 3%, 3mm (fig. 16a.) than plans 1(45) and 2(45). For gamma criteria of 2%, 2mm, plans 1 and 2 a have a lower pass rate than plan 3 (fig. 16b.).

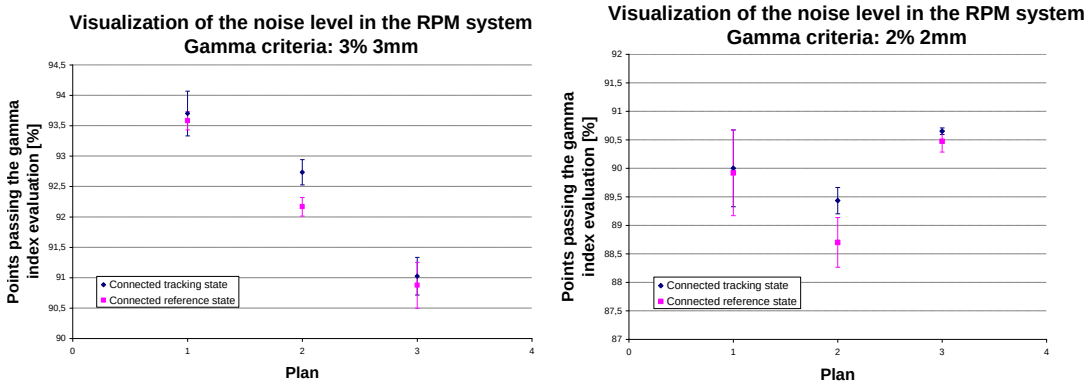

Figure 16a.-b. Visualization of the impact of RPM system on the tracking system when tracking a static target. Gamma index evaluation was made with a static target measurement in the disconnected state as reference using criterias 3%, 3mm and 2%, 2mm. Error bars = 1 SD

3.4.3. Temporal drift and noise level in the RPM system

The temporal drift of the performed measurements in the connected tracking state was in the range of 0.0063 mm/min to 0.015 mm/min (table. 7). An example of the 20 min acquisitions are shown in fig.17. The occurrence and the direction of the shifts appeared to be random. The temporal drift in the RPM system was found not to be large enough to have caused the shift in the dose profiles that were seen in the measurements in the connected tracking state.

The noise level of the RPM system was fairly consistent and the standard deviation was found to be slightly above 1 mm (table 7). The large standard deviation can be explained by the absence of temporal averaging (which is used for clinical monitoring of respiratory movements). The RPM system gives a positive output when the estimated marker block position is closer to the RPM camera than the calibration position and a negative output when the estimated position is further away from the camera than the calibration position.

Table 7 Investigation of RPM drift and noise level. Positive values implies positions closer to the RPM camera than the calibration position

Measurement	Drift in 1 min measurement [mm]	Mean drift [mm]	Standard deviation [mm]
1	0.0063	0.42	1.06
2	-0.0075	0.27	1.01
3	-0.015	-0.20	1.16
4	-0.0075	-0.49	1.11
5	0.015	0.35	1.06
6	-0.015	0.34	1.05

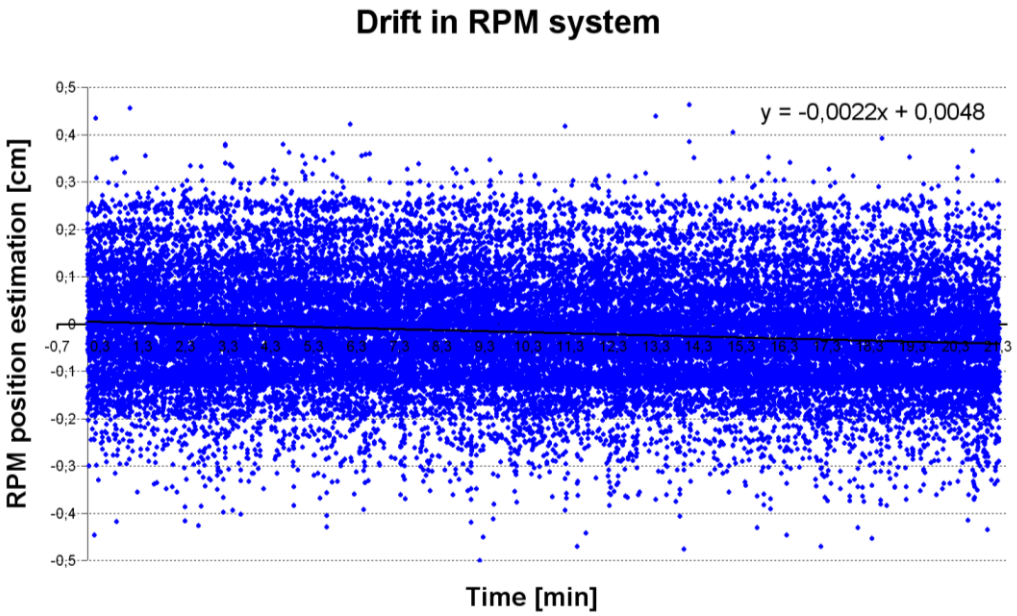

Figure 17 Example of an RPM measurement for investigation of the temporal drift and the system noise. Positive values implies positions closer to the RPM camera than the calibration position.

3.4.4 The ability of the RPM system to estimate the correct position of the marker block

The results showed a random error in the position estimation of the marker block. An example from the measurements is shown in fig. 18. Note that the estimation of the centre position is shifted in the opposite direction compared to the outer positions. This implies that the position estimation can be shifted in different directions for different displacement lengths after the same calibration of the system.

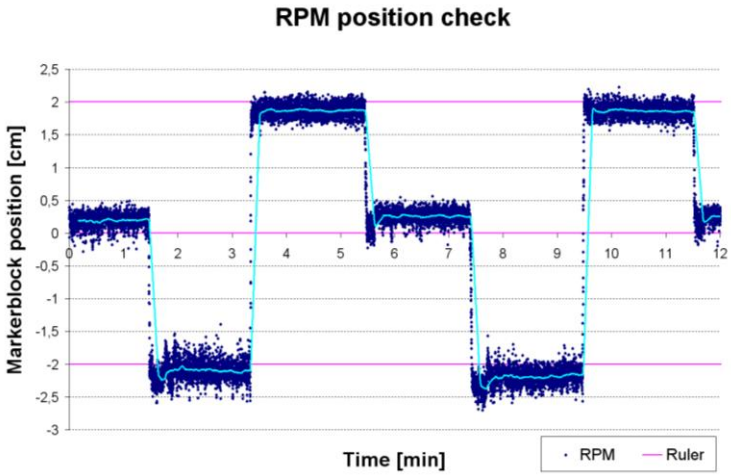

Figure 18 Example of measurement to investigate the accuracy of the RPM system's position estimation. The mean RPM position value is plotted as a light blue line. Positive values implies positions closer to the RPM camera than the calibration position.

The calculated means of the RPM position estimation are plotted together with the ruler measurements in fig. 19a.-d. There seems to be no clear trend in the error of the position estimation. When the marker block is moved towards the camera, the RPM displacement estimation is smaller than the ruler estimations for most of the measurements. When the marker block is moved away from the camera, the RPM system sometimes overestimates, and sometimes underestimates the displacement. For three of the measurements, the central position was estimated fairly accurately by the RPM system. For measurement c, however, the system estimated the marker block to be positioned closer to the camera than the actual position. The difference between the measurements 18 a.-d. are larger than the variations within the same measurements, which could explain why the profile shift of two measurements performed immediately after one another could be very different. The RPM position estimation appears to be fairly stable compared to the ruler measurements during the one hour measurements.

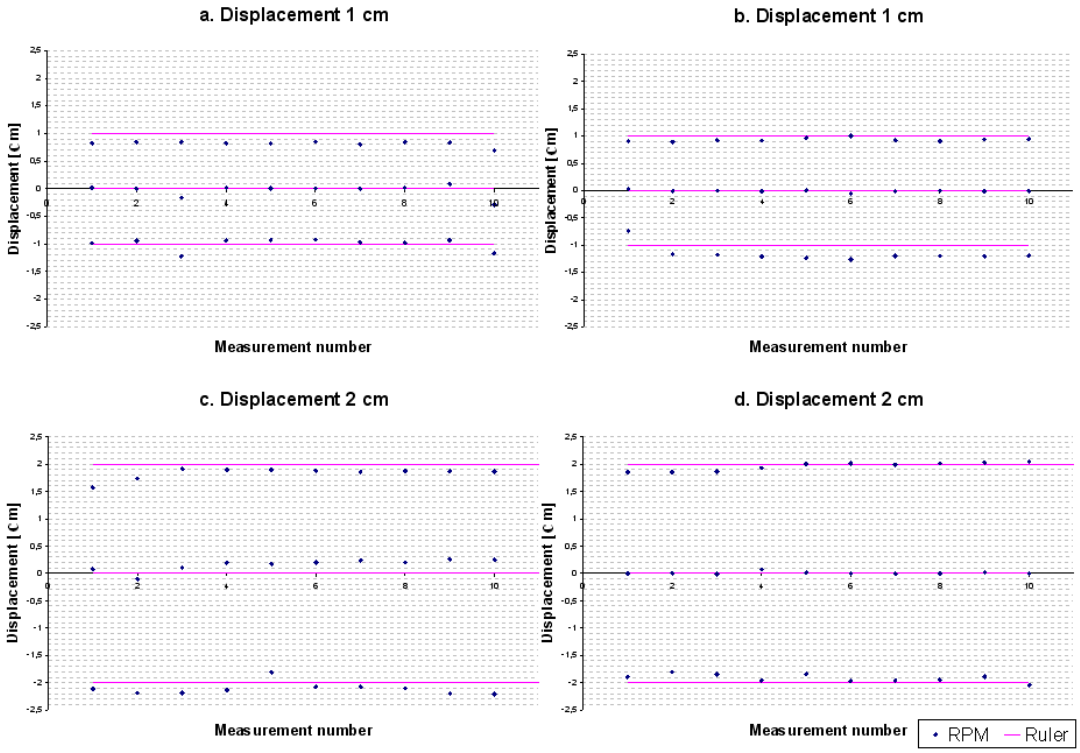

Figure 19a.-d. Mean position estimation of the RPM system compared to the positions measured with a ruler. Positive values implies positions closer to the RPM camera than the calibration position.

For the MLC tracking measurements, where the goal is solely to investigate the characteristics of the tracking controller, there might be a benefit in recalibrating the RPM system until finding a calibration that gives fairly accurate position estimation, and then to use this calibration for all of the measurements. The static measurement in the connected tracking state might then have the same profile shift as the rest of the measurements in this state and could be used as the reference measurement in the gamma index evaluation.

Another additional reason why the RPM system is not a favourable position monitoring device for DMLC tracking is that there is no sufficient correlation between the internal tumour movement and the movement of the external marker block. An accurate method to correlate these motions would be required in order to use the RPM monitoring system for DMLC tracking in the clinic.

The results of the investigation of the temporal drift in the RPM system and the system's ability to estimate the correct position of the marker block were supported by measurements performed by Varian Medical Systems [22].

3.5 Accuracy of the Respiratory gating platform

The accuracy of the respiratory gating platform is shown in table 11. The difference between the indicated and measured cycle time was found to be about 1 second which is quite a lot for a cycle time of about 6 seconds. However, studies [17] have shown that a lung tumour can have a cycle time of up to 6.6 s which makes a cycle time of about 7 seconds clinically relevant. The displacement accuracy of the

platform was found to be in the range of 0 to 1 mm depending on what length of peak-to-peak displacement used. The reproducibility of the platform movements were assumed to be good and not introducing any variations between the measurements in the different tracking states.

Table 11 Measured displacement and cycle time of the respiratory gating platform

Peak to peak displacement [mm]	Measured displacement [mm]	Difference between the indicated and real displacement [mm]	Measured cycle time [s]	Difference between the indicated and real cycle time [s]
5	4.5	-0.5	7.3	1.3
10	10.5	0.5	7.2	1.2
15	15	0	6.9	0.9
20	19	-1	6.8	0.8
25	24	-1	7.3	1.3
			Mean: 7.1	

3.6 MLC tracking method's effects on organs at risk

The DMLC tracking method has been shown to significantly improve the delivery accuracy to moving targets. Organs that move with the same amplitude and phase as the target (e. g. surrounding lung tissue) will clearly benefit from DMLC tracking since the method reduces the dose smearing and possibly enables margin reduction. Serial organs at risk that are static or not moving according to the target movements (e. g. the spinal cord) will most likely also benefit from DMLC tracking since the localization of the reduced PTV will vary during the delivery and result in smearing of the dose to the organ at risk.

4. Conclusion and future outlook

The dosimetric accuracy when treating a moving target is clearly degraded as the peak to peak amplitude increases when no motion compensation method is used. DMLC tracking can improve the delivery accuracy of inversely optimized arc radiotherapy for moving targets. The benefits of the method are more apparent when using gamma index criteria of 2%, 2mm than the more commonly used 3%, 3mm criteria which suggests that a very accurate dose delivery is possible with DMLC tracking. The DMLC tracking method is not significantly affected by the size of the peak to peak displacement. There is a weak trend towards better tracking performance with 90º than with 45º collimator angle.

DMLC tracking can possibly enable margin reduction as it reduces the dose smearing. The use of an RPM system, with the current characteristics, does not provide an adequate monitoring of the target position for DMLC tracking, due to intermittent instabilities of the system.

There is a strong need for a position monitoring device that provides correct information about the target position at all times. Several position monitoring devices are currently under investigation at Stanford University for potential use with DMLC tracking. One of them is the Calypso® 4D Localization System [23] that uses an electromagnetic array to excite transponders implanted in the tumour and to acquire the responding signal. The Calypso® 4D Localization System has the advantage that no ionizing radiation is used to localized the target. A problem with this system is that the transponders are thicker than gold markers currently used and are therefore difficult to implant in a tumour. The Calypso® 4D Localization system is still under development and it is not clinically used at the moment. [23] Another method being developed is position monitoring using frequently acquired x-ray images (kV and/or MV) of the target during the treatment delivery. This method would give additional radiation dose to the patient from the x-ray image exposures. A position monitoring device that has not yet been tested with DMLC tracking is the ExacTrac® system (BrainLAB) [24]. This system uses a combination of x-ray imaging and infrared tracking to estimate the position of the target. The use of the infrared tracking reduces the need for x-ray images during the delivery which is desirable. The ExacTrac® position monitoring system will be tested for DMLC tracking with RapidArc in the near future at Rigshospitalet.

Even though the measurements in this study were performed without the use of a prediction algorithm, the tracking performance was impressive. But since previous studies [8] have shown that reduction of the response time of the system would increase the over all accuracy, there is an urge to investigate the tracking performance when using a functioning prediction algorithm with RapidArc delivery.

Sinusoidal paths, as studied in this work, are good approximations for lung tumour movements, but when moving towards clinical applications, real patient specific tumour movements need to be considered. Studies of DMLC tracking for complex tumour movement in 3D are therefore required.

Acknowledgements

First of all, I would like to thank my supervisors, Per Munck af Rosenschöld and Stine Korreman for the opportunity to perform this work. Their great support and guidance have been indispensable during this project. I would also like to thank Varian Medical Systems and the MLC tracking research group at Stanford University for providing the MLC controller system and for all support and guidance. I would also like to express my gratitude to the MRRG research group at Rigshospitalet for useful input and to Dr Anders Ask for helping me with the delineation of organs at risk for the RapidArc plans. And finally, I would like to thank Jens Zimmerman and Marianne Aznar who took great time to help and support me during this project.

References

[1] *Yu CX, Jaffray DA, Wong JW, Martinez A*. Intensity modulated arc radiotherapy: a new method for delivering conformal treatments. Radiotherapy and Oncology. 1995;37:16

[2] *Otto K.* Volumetric modulated arc therapy: IMRT in a single gantry arc. Med Phys 2008;35:310-17

[3] *Cancerfonden:* http://www.cancerfonden.se/Global/dokument/omcancer/cancer_i_siffror/Cancer_i_siffror_2009.pdf

[4] *Wolthaus JWH, Schneider C, Snoke JJ, Herk MV, Belderbos JSA, Rossi MMG, Lebesque JV, Damen EMF*. Mid-ventilation CT scan construction from four-dimensional respiration-correlated CT scans for radiotherapy planning of lung cancer patients. Radiation Oncology Biol. Phys. 2006;65:1560-1571

[5] *Hernando ML, Marks LB, Bentel GC, Zhou SM, Hollis D, Das SK, Fan M, Munley MT, Shafman TD, Anscher MS, Lind PA.* Radiation-induced pulmonary toxicity: A dose- volume histogram analysis in 201 patients with lung cancer. Int. J. Radiation Oncology Biol. Phys.2001;51:650-659

[6] *Korreman S, Juhler-Nøttrup T, Boyer AL.* Respiratory gated delivery cannot facilitate margin reduction, unless combined with respiratory correlated image guidance. Radiotherapy and Oncology. 2008;86:61-68

[7] *Sawant A, Venkat R, Srivastava V, Carlson D, Povzner S, Cattell H, Keall P*. management of three-dimentional intra fraction motion through real-time DMLC tracking. Med Phys 2008;35:2050-61

[8] *Keall PJ, Cattell H, Pokhrel D, Dieterich S, Wong KH, Murphy MJ, Vedam SS, Wijesooriya K, Mohan R.* Geometric accuracy of a real-time target tracking system with dynamic multileaf collimator tracking system. Int. J. Radiation Oncology Biol. Phys.2006;65:1579-1584

[9] *Zimmerman J, Korreman S, Persson G, Cattell H, Svatos M, Sawant A, Venkat R, Carlsson D, Keall P.* DMLC motion tracking of moving targets for intensity modulated arc therapy treatment – a feasibility study. Acta Oncologica 2008:1-6

[10] *Varian Medical Systems*, Inc. 3100 Hansen Way. Palo Alto, CA 94304-1038

[11] *ScandiDos:* http://www.scandidos.se/?page_id=6&f=1_5_6

[12] *Varian Medical Systems, Inc:* http://www.varian.com/us/oncology/radiation_oncology/clinac/rpm_respiratory_gating.html

[13] *Varian Medical Systems, Inc:* http://www.varian.com/us/oncology/treatments/treatment_techniques/rapidarc/

[14] *Fogliata A, Clivio A, Nicolini G, Vanetti E, Cozzi L.* Intensity modulation with photons for benign intracranial tumours: A planning comparison of volumetric single arc, helical arc and fixed gantry techniques. Radiotherapy and Oncology 2008;89:254-262

[15] *Gagné I, Zavgorodni S.* Evaluation of the analytical anisotropic algorithm in an extreme water-lung interface phantom using Monte Carlo dose calculations. Journal of Applied Clinical Medical Physics 2007;8:33-46

[16] *MLC-tracking Research group:* Paul Keall, Byungchul Cho, Per Poulsen, Dan Ruan and Amit Sawant, Stanford University, Stanford, CA, USA

[17] *Seppenwoolde Y, Shirato H, Kitamura K, Shimizu S, Van Herk M, Lebesque JV, Miyasaka K.* Precice and real-time measurement of 3D tumour motion in lung due to breathing and heartbeat, measured during radio therapy. Radiation Oncology Biol. Phys 2002;53:822-834

[18] *Standard Imaging:* http://www.standardimaging.com/product_home.php?id=36&tab=specs

[19] *Low D, Harms W, Mutic S, Purdy J.* A thechnique for the quantitative evaluation of dose distributions. Med. Phys. 1998;25:656-661

[20] *Herk V M, Remeijer P, Rasch C, Lebesque JV.* The Probability of correct target dosage: Dose-population histograms for deriving treatment margins in radiotherapy. Int. J. Radiation Oncology Biol. Phys. 2000;47:1121-1135

[21] Ekberg L, Holmberg O, Wittgren et al. What margins should be added to the clinical target volume in radiotherapy treatment planning for lung cancer? Radiotherapy and Oncology 1998;48:71-77

[22] *Hassan Mostafavi*, Ginzton Technology CenterVarian Medical Systems, Inc. 2599 Garcia Avenue, Mountain View, CA 94043, USA

[23] *Calypso medical systems:* http://www.calypsomedical.com/HealthCareTechnology.aspx#first

[24] *BrainLab:* http://www.brainlab.com/scripts/website_english.asp?menuDeactivate=0&articleID=2646&articleTypeID=67&pageTypeID=4&article_short_headline=ExacTrac®%20IGRT%20General%20Overview

Appendix I

Table 12 Results of the gamma index evaluation

Gamma 2% 2mm

Plan	Peak to peak displacement [mm]	Connected tracking state		Disconnected state		Number of measurements	
		Mean of % Points passing evaluation	SD	Mean of % Points passing evaluation	SD	Connected tracking state	Disconnected state
1	5	97.1	5.4	96.5	6.2	6	5
	10	91.0	15.3	85.7	19.6	5	5
	15	95.8	7.0	71.5	19.1	5	5
	20	94.5	10.4	52.7	14.9	6	5
	25	88.3	16.0	40.6	10.8	4	5
2	5	99.3	0.6	99.8	0.2	3	3
	10	96.5	0.2	93.5	2.0	2	3
	15	98.5	0.6	80.5	1.5	2	3
	20	95.5	2.3	59.6	3.5	2	3
	25	94.6	-	49.4	1.8	1	3
3	5	100.0	0.0	98.5	1.6	4	4
	10	99.8	0.3	88.6	1.1	3	4
	15	99.8	0.3	77.7	3.2	3	4
	20	98.4	2.4	55.0	3.7	3	4
	25	98.5	2.1	38.9	3.3	4	4

Gamma 3% 3mm

Plan	Peak to peak displacement [mm]	Connected tracking state		Disconnected state		Number of measurements	
		Mean of % Points passing evaluation	SD	Mean of % Points passing evaluation	SD	Connected tracking state	Disconnected state
1	5	99.1	2.3	98.8	2.6	6	5
	10	95.3	9.7	91.2	14.8	5	5
	15	98.4	3.6	87.4	21.5	5	5
	20	97.6	5.7	79.6	21.9	6	5
	25	94.9	9.4	64.8	20.5	4	5
2	5	99.9	0.2	100.0	0.0	3	3
	10	99.6	0.2	98.0	0.8	2	3
	15	99.9	0.2	97.6	0.5	2	3
	20	99.3	0.6	86.4	0.6	2	3
	25	99.2	-	76.2	2.1	1	3
3	5	100.0	0.0	99.9	0.2	4	4
	10	100.0	0.0	93.3	1.7	3	4
	15	100.0	0.0	91.8	1.3	3	4
	20	100.0	0.0	85.1	0.8	3	4
	25	100.0	0.0	69.8	1.6	4	4

Table 13 Results of the dose deviation evaluation

Dose deviation 2%

Plan	Peak to peak displacement [mm]	Connected tracking state		Disconnected state		Number of measurements	
		Mean of % Points passing evaluation	SD	Mean of % Points passing evaluation	SD	Connected tracking state	Disconnected state
1	5	73.7	19.2	89.4	7.1	6	5
	10	73.4	16.7	59.9	20.8	5	5
	15	73.4	18.5	45.1	19.3	5	5
	20	74.6	14.4	36.1	14.2	6	5
	25	74.2	13.2	24.4	12.1	4	5
2	5	82.6	8.8	86.0	5.1	3	3
	10	71.0	3.7	47.8	2.1	2	3
	15	82.4	4.2	36.7	1.4	2	3
	20	60.9	14.9	25.3	1.7	2	3
	25	61.9	-	21.7	0.7	1	3
3	5	75.0	11.6	70.5	5.2	4	4
	10	66.5	6.6	35.1	3.9	3	4
	15	77.6	10.4	24.0	2.7	3	4
	20	55.7	24.6	18.6	2.1	3	4
	25	58.5	16.7	8.8	2.6	4	4

Dose deviation 3%

Plan	Peak to peak displacement [mm]	Connected tracking state		Disconnected state		Number of measurements	
		Mean of % Points passing evaluation	SD	Mean of % Points passing evaluation	SD	Connected tracking state	Disconnected state
1	5	84.7	12.9	94.8	4.2	6	5
	10	84.8	11.1	73.5	14.7	5	5
	15	84.1	13.0	60.4	21.5	5	5
	20	85.8	9.7	52.1	24.2	6	5
	25	86.7	9.0	38.5	20.7	4	5
2	5	90.4	5.7	92.5	4.1	3	3
	10	85.9	5.0	62.5	2.0	2	3
	15	94.0	2.8	51.0	1.3	2	3
	20	77.8	11.6	36.8	1.6	2	3
	25	81.6	-	30.7	2.1	1	3
3	5	85.4	6.7	83.1	4.9	4	4
	10	79.2	5.3	48.5	3.5	3	4
	15	89.5	4.9	36.2	0.7	3	4
	20	69.9	15.9	25.8	3.2	3	4
	25	72.9	13.1	15.4	3.7	4	4

Table 14 Results of the distance to agreement evaluation

DTA 2mm

Plan	Peak to peak displacement [mm]	Connected tracking state		Disconnected state		Number of measurements	
		Mean of % Points passing evaluation	SD	Mean of % Points passing evaluation	SD	Connected tracking state	Disconnected state
1	5	98.3	2.9	99.9	0.3	6	5
	10	98.7	1.5	98.1	0.6	5	5
	15	99.3	1.1	91.6	4.0	5	5
	20	99.5	0.5	72.4	1.6	6	5
	25	99.1	0.9	58.4	2.6	4	5
2	5	99.2	0.8	99.8	0.3	3	3
	10	98.5	1.4	97.6	1.8	2	3
	15	99.5	0.8	88.6	2.5	2	3
	20	98.2	2.5	73.1	2.4	2	3
	25	99.0	-	60.7	1.8	1	3
3	5	100.0	1.3	99.4	1.2	4	4
	10	99.5	2.3	94.1	4.9	3	4
	15	100.0	0.0	88.4	5.2	3	4
	20	99.3	2.9	73.9	5.3	3	4
	25	98.4	2.5	55.9	7.0	4	4

DTA 3mm

Plan	Peak to peak displacement [mm]	Connected tracking state		Disconnected state		Number of measurements	
		Mean of % Points passing evaluation	SD	Mean of % Points passing evaluation	SD	Connected tracking state	Disconnected state
1	5	99.9	0.2	100.0	0.0	6	5
	10	100.0	0.0	99.7	0.5	5	5
	15	99.8	0.3	98.8	0.8	5	5
	20	99.9	0.2	94.3	2.9	6	5
	25	99.8	0.3	81.3	3.7	4	5
2	5	99.7	0.3	99.8	0.3	3	3
	10	99.5	0.0	99.6	0.3	2	3
	15	100.0	0.0	97.8	1.2	2	3
	20	100.0	0.0	90.0	1.1	2	3
	25	100.0	-	81.1	1.7	1	3
3	5	100.0	0.0	100.0	0.0	4	4
	10	100.0	0.0	96.4	1.7	3	4
	15	100.0	0.0	95.5	1.3	3	4
	20	100.0	0.0	91.6	1.2	3	4
	25	99.9	0.3	78.6	2.8	4	4

Appendix II

Investigation of the influences of the RPM system

RPM systems influence on the tracking performance with a static target

Table 15 Estimation of RPM systems influence on the tracking performance with a static target. Gamma index evaluation (3%, 3mm) with a static target measurement in the disconnected state as reference was used and the mean and standard deviation for the measured plans were calculated. The number of measurements used in this evaluation are 5 (plan 1(45)), 3 (plan 2(45)) and 4 (plan 3(90)).

	Plan 1(45)		Plan 2(45)		Plan 3(90)	
	Mean	SD	Mean	SD	Mean	SD
Connected tracking state	96.0	0.7	95.4	0.8	97.1	0.4
Connected reference state	93.6	92.2	90.9	0.1	0.2	0.4

Table 16 Estimation of RPM systems influence on the tracking performance with a static target. Gamma index evaluation (2%, 2mm) with a static target measurement in the disconnected state as reference, was used and the mean and standard deviation for the measured plans were calculated. The number of measurements used in this evaluation are 5 (plan 1(45)), 3 (plan 2(45)) and 4 (plan 3(90)).

	Plan 1(45)		Plan 2(45)		Plan 3(90)	
	Mean	SD	Mean	SD	Mean	SD
Connected tracking state	92.7	0.9	92.9	0.4	96.1	0.5
Connected reference state	89.9	0.7	88.7	0.4	90.5	0.2

RPM systems ability to estimate the correct position of the marker block

Table 17 Displacement deviation between the RPM measurements and the position measured with a ruler

	Deviation [cm] of measurements with displacement length				Deviation [cm] of measurements with displacement length		
	0 cm	1 cm	-1 cm		0 cm	2 cm	-2 cm
a	0.02	-0.17	0.02	c	0.08	-0.43	-0.11
	0.01	-0.15	0.06		-0.10	-0.27	-0.19
	-0.16	-0.15	-0.22		0.10	-0.09	-0.19
	0.02	-0.17	0.06		0.20	-0.10	-0.13
	0.01	-0.18	0.07		0.17	-0.10	0.19
	0.00	-0.15	0.08		0.20	-0.12	-0.07
	0.01	-0.19	0.04		0.24	-0.14	-0.07
	0.02	-0.15	0.02		0.20	-0.13	-0.10
	0.09	-0.16	0.07		0.26	-0.14	-0.20
	-0.29	-0.31	-0.17		0.25	-0.14	-0.21
b	0.03	-0.09	0.26	d	0.00	-0.15	0.11
	-0.01	-0.10	-0.17		0.01	-0.15	0.20
	0.00	-0.07	-0.17		-0.01	-0.14	0.15
	-0.01	-0.08	-0.21		0.07	-0.07	0.04
	0.00	-0.04	-0.23		0.01	0.00	0.16
	-0.05	0.00	-0.26		0.00	0.01	0.03
	-0.01	-0.07	-0.19		0.00	-0.01	0.04
	0.00	-0.09	-0.20		0.00	0.01	0.05
	-0.01	-0.06	-0.20		0.02	0.02	0.11
	0.00	-0.06	-0.19		0.00	0.04	-0.04

Table 18 Properties of the displacement deviation between the RPM measurements and the position measured with a ruler

	Mean [cm] of deviation of measurements with displacement length			Max [cm] of deviation of measurements with displacement length			Min [cm] of deviation of measurements with displacement length			SD of deviation of measurements with displacement length		
	0 cm	1 cm	-1 cm	0 cm	1 cm	-1 cm	0 cm	1 cm	-1 cm	0 cm	1 cm	-1 cm
a	-0.03	-0.18	0.00	0.09	-0.15	0.08	-0.29	-0.31	-0.22	0.11	0.05	0.11
b	-0.01	-0.07	-0.16	0.03	0.00	0.26	-0.05	-0.10	-0.26	0.02	0.03	0.15
	0 cm	2 cm	-2 cm	0 cm	2 cm	-2 cm	0 cm	2 cm	-2 cm	0 cm	2 cm	-2 cm
c	0.16	-0.17	-0.11	0.26	0.00	0.00	-0.10	0.00	0.00	0.11	0.00	0.00
d	0.01	-0.04	0.09	0.07	0.04	0.20	-0.01	-0.15	-0.04	0.02	0.08	0.07

Appendix III

Technical specifications

Table 19 Technical specifications for Scandidos Delta4 [11]

Cylinder phantom material	PMMA
Calibration phantom material	PMMA
Detectors Type	p-Si
Total number of detectors	1069
Maximum deviation of detector position relative to markings on the phantom	0.5 mm
Detection area per plane	20 x 20 cm
Distance between detectors, central area (6 x 6 cm)	5 mm
Distance between detectors, outer area (20 x 20 cm)	10 mm
Size	0.78 mm^2
Shape	Cylindrical
Dose range	From 1 mGy to unlimited
Resolution	0.01 mGy
Sensitivity decrease (in a 10 MeV electron beam)	1 %/kGy
Cylinder diameter	22 cm
Cylinder length	40 cm
Total length	72 cm
Total weight	27 kg

Table 20 Specifications for the Respiratory gating platform [18]

Height	12.7 cm
Width	30.5 cm
Length	76.2 cm
Weight	9.1 kg
Period of Oscillation Control	2 – 6 sec, 0.5 sec increments
Accuracy	± 0.2 second when using: 4 Standard Imaging IMRT Phantom slabs (~34 lbs.) 6 Standard Imaging IMRT Phantom slabs (~51 lbs.) 8 Standard Imaging IMRT Phantom slabs (~68 lbs.)
Repeatability	± 0.1 second for 4, 6 or 8 Standard Imaging IMRT Phantom slabs
Range of Motion Control	5 mm - 40 mm, with 5 mm increments
Accuracy and Repeatability	± 0.5 mm
Power Requirements	12 VDC @ 1.25 A, power supply included
DC Output	Use only Globtek®, Inc power supply model GTM21089-1512-T3
Weight capacity	15.4-30.8 kg

Table 21 Technical specifications for PTW Seven29 detector array [25]

Number of chambers	729
Detector type	Vented ionization chambers
Max fiels size	27 cm x 27 cm
Chamber size	5 mm x 5 mm x 5mm (0.125 cm3)
Chamber arrangement	Matrix of 27 x 27 chambers (10 mm centre to centre)
Dead time	Zero
Repetition time	200 ms
Measured quantities	Absorbed dose to water (Gy), Absorbed dose rate to water (Gy/min)
Resolution	1 mGy or 1 mGy/min
Measurement range	(0.5 ... 12) Gy/min
Reference point	5 mm below the surface of the array
Housing material	PMMA
Dimensions	300 mm x 420 mm x 22 mm (W x D x H)
weight	Approx. 3.2 kg